

Direct and Large Eddy Simulation of a turbulent channel flow with roughness on one wall.

S. Leonardi¹, F. Tessicini², P. Orlandi¹ and R.A. Antonia³

¹Dipartimento di Meccanica e Aeronautica
Università La Sapienza, Via Eudossiana 16, I-00184, Roma

²Dep. of Aer. Imperial College of London
London UK

³Discipline of Mechanical Engineering,
University of Newcastle, NSW 2308 Australia

Abstract

Large and Direct Numerical Simulations (LES, DNS) of a turbulent channel flow with square bars on one wall have been carried out at $Re = 10400$. Two sub-grid models have been used: Smagorinsky with Van Driest damping and Dynamic. There is satisfactory agreement between the two types of simulations for the pressure and skin friction on the wall and the *rms* streamwise velocity. Comparison for the *rms* normal and spanwise velocities is poor but the sub-grid models are a significant improvement relative to the no model (which corresponds to an unresolved DNS). A further DNS at $Re = 18000$ has been performed with the aim of comparing the results with the experiment by Hanjalic & Launder [1]. The Reynolds number dependence (Re ranging from 4200 to 18000) has been discussed. The pressure on the wall and hence the form drag does not depend on Re and the velocity profile changes slightly for $Re > 10400$.

Introduction

Flows over rough surfaces are of interest in many practical applications, ranging from shipbuilding and aviation, the flows over blades in different types of turbomachines and the flows over vegetated surfaces in the atmospheric surface layer. In all these cases, the Reynolds number is high and the roughness is very small relative to the characteristic length of the outer flow. Jiménez [2] claimed that numerical or laboratory experiments should have at least $\delta/k > 50$ and $k^+ = ku\tau/\nu$ in the fully rough regime (δ represents either the diameter of the pipe, the thickness of the boundary layer or the half-width of a duct, and k^+ is the height of the roughness elements in wall units). Therefore, numerical simulations require a large number of points. For this reason, to date, numerical simulations have been carried out only at low Reynolds numbers ($Re = U_c h/\nu < 10000$, h is the channel half-width, U_c is the centerline velocity and ν is the kinematic viscosity) e.g. DNS, [3], [4], [5] and LES, [6]. Although these simulations have provided useful results, it is important to increase the Reynolds number. In the present paper, LES and DNS results of a turbulent channel flow with square bars on the bottom wall and a smooth upper wall are discussed. One of the aims is to compare the results with those of the experiment by Hanjalic & Launder [1] for a turbulent channel flow with square bars on the bottom wall with $\lambda/k = 10$, where λ is the distance between successive elements. DNSs have been carried out at $Re = 10400$ and $Re = 18000$. The computational box is $8h \times 2.125h \times 6.25h$ in the streamwise (x) wall-normal (y) and spanwise (z) direction respectively. The additional $0.125h$ increase in the channel height is due to the cavity height where the square elements ($k = 0.125h$) are placed. In this context, the development of reliable LES sub-grid models remains an important objective.

The grid used for the LES, ($240 \times 160 \times 49$ in x, y, z respectively), is much coarser than that used for the DNS ($513 \times 177 \times 193$ and $769 \times 161 \times 193$ for $Re = 10400$ and $Re = 18000$ respectively). The models used are the standard Smagorinsky model with Van Driest damping ($C_s = 0.1$, hereafter SM10) and the dynamic model (DYN). To underline the effect of the sub-grid model, a simulation without model has been carried out (NOM). The latter would correspond to an unresolved DNS.

Numerical Procedure

The non-dimensional Navier-Stokes and continuity equations for incompressible flows are:

$$\frac{\partial U_i}{\partial t} + \frac{\partial U_i U_j}{\partial x_j} = -\frac{\partial P}{\partial x_i} + \frac{1}{Re} \frac{\partial^2 U_i}{\partial x_j^2} + \Pi, \quad \nabla \cdot U = 0 \quad (1)$$

where Π is the pressure gradient required to maintain a constant flow rate, U_i is the component of the velocity vector in the i direction and P is the pressure. The Navier-Stokes equations have been discretized in an orthogonal coordinate system using the staggered central second-order finite-difference approximation. Here, only the main features are recalled since details of the numerical method can be found in Orlandi [7]. The discretized system is advanced in time using a fractional-step method with viscous terms treated implicitly and convective terms explicitly. The large sparse matrix resulting from the implicit terms is inverted by an approximate factorisation technique. At each time step, the momentum equations are advanced with the pressure at the previous step, yielding an intermediate non-solenoidal velocity field. A scalar quantity Φ projects the non-solenoidal field onto a solenoidal one. A hybrid low-storage third-order Runge-Kutta scheme is used to advance the equations in time. The roughness is treated by the efficient immersed boundary technique described in detail by Fadlun *et al.* (2000). This approach allows the solution of flows over complex geometries without the need of computationally intensive body-fitted grids. It consists of imposing $U_i = 0$ on the body surface which does not necessarily coincide with the grid. Another condition is required to avoid that the geometry is described in a stepwise way. Fadlun *et al.* (2000) showed that second-order accuracy is achieved by evaluating the velocities at the closest point to the boundary using a linear interpolation. This is consistent with the presence of a linear mean velocity profile very near the boundary even for turbulent flows, albeit at the expense of clustering more points near the body.

Results and discussion

The square element on the bottom wall induces a separation at the trailing edge of the elements ($x/k \simeq 1$ Fig.1). In agreement with the results of Leonardi *et al.* [4] obtained for larger ele-

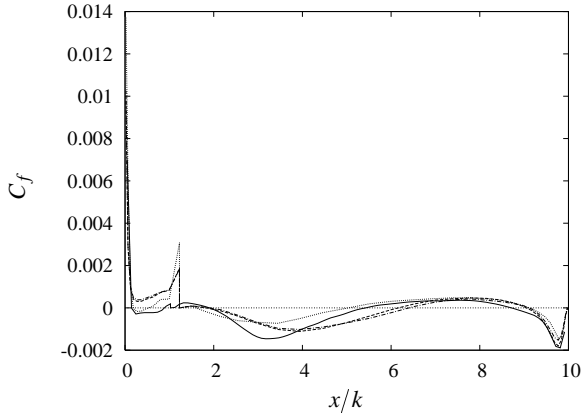


Figure 1: Frictional drag on the horizontal walls of a roughness element at $Re = 10400$. — DNS, NOM, - - - Smagorinsky, - · - Dynamic.

ments (DNS $k = 0.2h$) the flow reattaches on the bottom wall at about $x/k \simeq 5$ (where $x = 0$ is taken at the leading edge of the element). On the other hand, LES simulations predict a larger recirculating region, with a smaller intensity. As the next element is approached, a separation occurs at about $x/k \simeq 9$, one roughness height upstream of the element. The LESs, in this case, yield a good approximation for the C_f with respect to the DNS. This behaviour is due to the non-uniform grid used for the LES with a larger number of points very near the element, and a very coarse resolution within the cavity. The element leads to a large increase of velocity and a presence of the friction peak at the leading edge of the element. Above the crest, as shown in Leonardi *et al.* [4] for $\lambda/k > 8$ a separation occurs. LES and NOM are not able to reproduce this separation which was also observed in the experiment of Liu, Kline and Johnston [9].

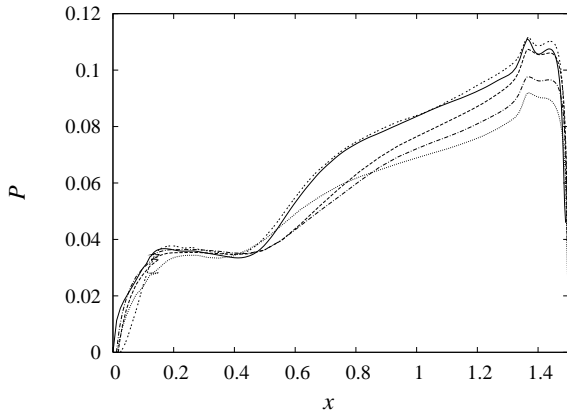


Figure 2: Pressure along the walls of a roughness wavelength. $Re = 10400$: — DNS, NOM, - - - Smagorinsky, - · - Dynamic. $Re = 18000$ DNS.

Pressure distributions along the horizontal and vertical walls are shown in Fig. 2 over one wavelength. Very near the element ($0 < x < 0.25$ and $1.25 < x < 1.5$) LES and DNS results are in good agreement. At the center of the cavity, larger differences are found. This is again due to the non-uniform grid used. Since the difference between pressure distributions on the vertical walls, corresponds to the form drag for this roughness element, approximately, the LES and DNS yield values of the form drag that agree. On the other hand, NOM yields a different pressure distribution over most of the wavelength and

a different (smaller) form drag. The pressure distributions for $Re = 10400$ and $Re = 18000$ are close to each other. The form drag, is $\overline{P}_d = 6.46E - 03$ and $6.6E - 03$ for $Re = 10400$ and $Re = 18000$ respectively ($\overline{P}_d = \lambda^{-1} \int_0^\lambda \langle P \rangle \vec{n} \cdot \vec{x} ds$, angular brackets denote averaging in time and z). This is an extension of the results of Leonardi *et al.* [4]. In a previous paper, they defined $C_d = \overline{P}_d/k$ and showed that for several values of λ/k , C_d does not depend on Re (which was varied between $Re = 4200$ to $Re = 10400$) and on k (in the range $0.1h$ to $0.2h$). For large values of λ/k (e.g. $\lambda/k > 3$), the total drag is almost entirely due to the form drag. Therefore, the value of the friction velocity, $U_\tau \equiv (\overline{P}_d + \overline{C}_f)^{1/2}$, does not change with the Reynolds number, ($\overline{C}_f = \lambda^{-1} \int_0^\lambda \langle C_f \rangle ds$). As a consequence, we believe that, for this type of roughness, the flow physics near the wall can be investigated through numerical simulations at moderate Reynolds numbers.

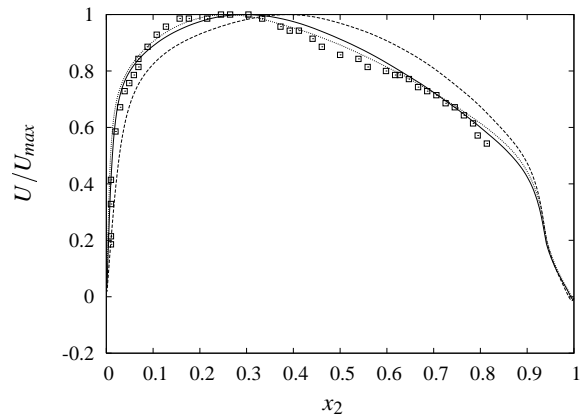


Figure 3: Mean velocity distribution. Symbols, experiment by Hanjalic & Launder [1], lines DNS. - - - $Re = 4200$, — 10400, 18000.

The mean velocity distribution shown in figure 3 for different Reynolds numbers, are compared with the measurements of Hanjalic & Launder [1] at $Re = 18000$. The agreement between experiment and DNS is satisfactory. The DNS results show that by increasing Re the maximum velocity is shifted upwards (towards the smooth wall). However, whereas the changes to the velocity profile are large between $Re = 4200$ and $Re = 10400$, only slight differences are observed between $Re = 10400$ and $Re = 18000$. Therefore, the dependence on the Reynolds number, for intermediate values of Re is weak even in the outer layer, so that DNS is a useful tool for providing insight into rough flows.

The velocity profile in wall units is:

$$U^+ = \kappa^{-1} \ln y^+ + C - \Delta U^+, \quad (2)$$

where C and κ are constants and "+" denotes normalization by either U_τ or v/U_τ . The origin for y is at $0.15k$ above the bottom wall. With respect to the smooth wall the velocity profile is shifted downward by a factor ΔU^+ , known as the roughness function. In Figure 4, the mean velocity profiles in wall units for DNS, LES and NOM are compared to the smooth wall distribution by Moser, Kim & Mansour [10]. As expected, the mean velocity profile is shifted downward, and the agreement between LES and DNS is reasonable. The roughness function is indeed due essentially to the increase of U_τ . For this value of λ/k , U_τ is mostly due to the pressure distribution which was shown to be similar for DNS and LES (Fig.2). On the other hand, the pressure drag for NOM was different from that relative to the DNS,

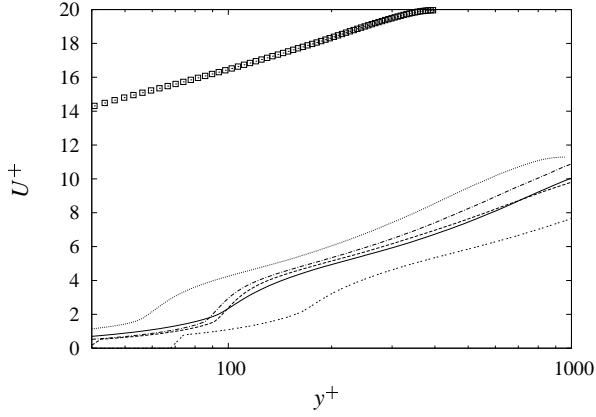


Figure 4: Mean velocity distribution in wall units. Symbols smooth channel Moser, Kim & Mansour [10], $Re = 10400$: — DNS, NOM, ---- Smagorinsky, -.-.- Dynamic. $Re = 18000$: DNS.

then larger differences to the velocity profile are expected. Even if U_τ does not change, the roughness function for $Re = 18000$ is larger than that for $Re = 10400$. As the origin in y is the same, and k^+ increases, the velocity distribution is shifted downward. In fact, Perry, Schofield & Joubert [11] showed that, for large λ/k (k-type roughness),

$$\Delta U^+ = \kappa^{-1} \ln k^+ + B. \quad (3)$$

The value of k^+ is 80, 103 and 180 for $Re = 4200$, 10400 and $Re = 18000$ respectively. The corresponding values of ΔU^+ are 12.9, 13.5 and 14.8 respectively, in agreement with equation 3 and $B = 2.2$. For these values of k^+ we are in the fully rough regime (Bandyopadhyay [12]).

Turbulent intensities are shown in Figure 5. For $\langle uu \rangle$, both the Large Eddy Simulations performed with Smagorinsky and dynamic models agree reasonably well with the DNS. However, for the other two stresses, the agreement is poor, especially for $\langle ww \rangle$. Near the rough wall ($x_2 = -1$), there is reasonable agreement for $\langle vv \rangle$ but significant differences can be discerned in the inner part of the channel. Perhaps surprisingly, the agreement between DNS and LES is not satisfactory near the upper smooth wall. Since sub-grid models work well for a smooth wall, this result should mean that the grid is too coarse to simulate the interaction between the two walls. In fact, roughness increases the communication between the wall and the outer layer. The improvement brought by the sub-grid models that have been tried is encouraging. Indeed, with respect to NOM, Large Eddy Simulations compare much better with the DNS results. While $\langle uu \rangle$ on the rough-wall is about the same as that on the smooth wall, $\langle vv \rangle$ and $\langle ww \rangle$ increase by about 2.5 times. This means that isotropy is better approximated over rough wall, as noted by Smalley *et al.* [13].

DNS results at $Re = 18000$ are compared with the experiment of Hanjalic & Launder [1] in Fig.6. Despite the uncertainty in the determination of U_τ the agreement is reasonable. In particular, $\langle uu \rangle$ and $\langle ww \rangle$ are in reasonable agreement, while there is poor agreement for $\langle vv \rangle$, especially near the wall.

Conclusions

Direct and Large Eddy Simulations have been performed for a turbulent channel flow with square bars on the bottom wall with a pitch to height value of $\lambda/k = 10$ at $Re = 10400$. For the pressure, skin friction and *rms* streamwise velocity the agreement between DNS and LES is satisfactory. On the other hand, for

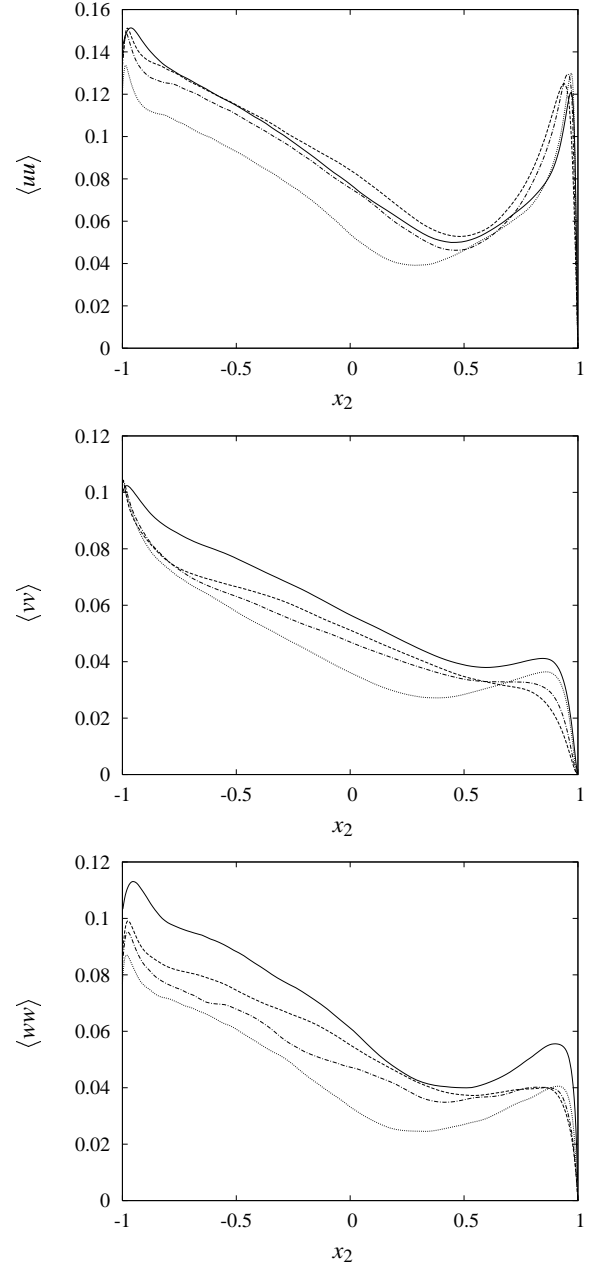


Figure 5: Normal turbulent intensities, $Re = 10400$: — DNS, NOM, ---- Smagorinsky, -.-.- Dynamic.

the *rms* spanwise and normal velocity, the agreement is poor. The improvement brought by the sub grid model is encouraging. The DNS at $Re = 18000$ showed a reasonable agreement with experimental results by Hanjalic & Launder [1]. The Reynolds number dependence for intermediate Reynolds is very weak, then we speculate that DNS can be very useful in the study of rough flows.

Acknowledgments

We acknowledge the support of the Australian Research Council, and the Ministero dell' Istruzione, dell' Università e della Ricerca and Centro di Eccellenza di Meccanica Computazionale, Politecnico di Bari.

References

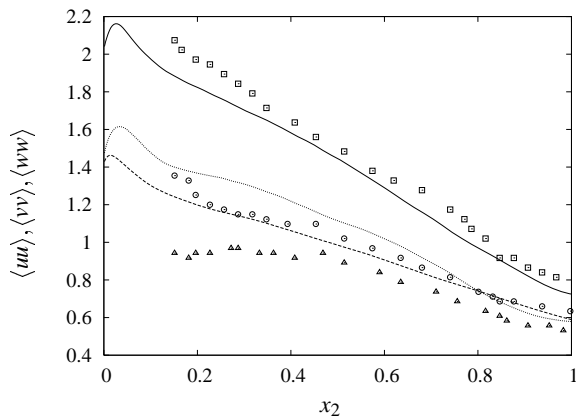


Figure 6: rms velocity fluctuation in wall units. Lines DNS at $Re = 18000$, symbols experiment by Hanjalic & Launder [1]: \square $\langle uu \rangle$, \triangle $\langle vv \rangle$, \circ $\langle ww \rangle$.

- [1] Hanjalic & Launder. Fully developed asymmetric flow in plane channel. *J. Fluid Mech.* **51**, 1972, 301–335.
- [2] Jiménez, J. Turbulent flows over rough walls. *Ann. Rev. Fluid Mech.* **36**, 2004, 173–196.
- [3] Miyake Y., Tsujimoto K. & Nagai N. Numerical simulation of channel flow with a rib-roughened wall. *J. Turb.* **3**, 2002, 35.
- [4] Leonardi, S., Orlandi, P., Smalley, R.J., Djenidi, L. & Antonia, R.A. Direct numerical simulations of turbulent channel flow with transverse square bars on one wall. *J. Fluid Mech.* **491**, 2003, 229–238.
- [5] Ashraffian A. & Anderson H.I. (2003). DNS of Turbulent Flow in a Rod-Roughened Channel. Proceedings of the Turbulent and Shear Flow Phenomena 3, Sendai, Japan. N. Kasagi, J. K. Eaton, R. Friedrich, J. A. C. Humphrey, M. A. Leschziner, T. Miyauchi. **Vol I**, 2003, 117–123.
- [6] Cui J., Virendra C. Patel & Ching-Long Lin. Large-eddy simulation of turbulent flow in a channel with rib roughness. *Int. J. of Heat and Fluid Flow* **24**, 2003, 372–388.
- [7] Orlandi, P. Fluid flow phenomena, a numerical toolkit. *Kluwer Academic Publishers*. 2000.
- [8] Fadlun E.A., Verzicco, R., Orlandi P. & Mohd-Yusof, J. Combined immersed boundary finite-difference methods for three-dimensional complex flow simulations. *J. Comput. Phys.* **161**, 2000, pp.35–60.
- [9] Liu, C.K., Kline, S.J. and Johnston, J.P. An experimental study of turbulent boundary layers on rough walls. Report MD-15, 1966, Department of Mechanical Engineering, Stanford University.
- [10] Moser R.D., Kim J. & Mansour N.N. Direct numerical simulation of turbulent channel flow up to $Re_\tau = 590$. *Phys. Fluids* **11**, 1999, 943–945.
- [11] Perry, A. E., Schofield, W. H. & Joubert, P. N. Rough wall turbulent boundary layers. *J. Fluid Mech.* **37**, 1969, 383–413.
- [12] Bandyopadhyay, P.R. Rough-wall turbulent boundary layers in the transition regime. *J. Fluid Mech.* **180**, 1987, pp.231–266.

- [13] Smalley, R.J., Leonardi, S., Antonia, R., Djenidi, L. & Orlandi, P. Reynolds stress anisotropy of turbulent rough walls layers. *Expts in Fluids* **33**, 2002, 31–37.